Anuário do Instituto de Geociências - UFRJ
www.anuario.igeo.ufrj.br

Biostratigraphy and Paleoecological Inferences Based on Oligocene Calcareous Nannofossils from the Ceará Rise (ODP Leg 154, Site 929A): Equatorial Atlantic Ocean

Bioestratigrafia e Inferências Paleoecológicas com Base em Nanofósseis Calcários Oligocênicos da Elevação Ceará (ODP Leg 154, Site 929A): Oceano Atlântico Equatorial

Anaiza Claudia Meira Devellard Fionda[1]; André Luiz Gatto Motta[2];
Claudia Maria Magalhães-Ribeiro[1]; Flávia Azevedo Pedrosa Lemos[3] & Maria Dolores Wanderley[2]

[1]Universidade Federal Rural do Rio de Janeiro, Instituto de Agronomia,
Departamento de Geociências, Rodovia BR 465, Km7, s/n, 23890-000, Seropédica, RJ, Brasil
[2]Universidade Federal do Rio de Janeiro, Instituto de Geociências, Departamento de Geologia,
Laboratório de Biossedimentologia e Nanofósseis Calcários,
Avenida Athos da Silveira Ramos, 274, 21910-916, Cidade Universitária, Ilha do Fundão, Rio de Janeiro-RJ, Brasil
[3]Universidade Federal de Pernambuco, Centro de Tecnologia e Geociências, Departamento de Geologia,
Laboratório de Bioestratigrafia Aplicada ao Petróleo, R. Acadêmico Hélio Ramos, s/n, 50740-467, Recife, PE, Brasil
E-mails: anaizaclaudiadevellard@outlook.com; andregatto@geologia.ufrj.br;
cmmagalhaesribeiro@gmail.com; flaviapedrosa.geo@gmail.com; doloreswanderley@msn.com
Recebido em: 10/09/2019 Aprovado em: 24/11/2019
DOI: http://dx.doi.org/10.11137/2020_1_07_17

Abstract

The Ceará Rise is an aseismic feature located in the Equatorial Atlantic Ocean, between the Amazon Cone, Demerara Abyssal Plain and the Ceará Abyssal Plain, which represents a key area for the understanding of deep ocean facies. In the oil and gas field, the identification of calcareous nannofossil-based biozones is important for the age modeling and comprehension of depositional evolution of the sedimentary strata. The study of Oligocene calcareous nannofossil-based succession at the Ceará Rise helped to detect paleoecological trends during the Oligocene. Using a polarized light optical microscope, forty-four species were observed, described and accounted in fifteen samples. The biostratigraphic model includes the standard biozones NP23, NP24 and NP25, as well as the recently proposed biozone NP26 - *Clausicoccus fenestratus*. Among the species found, *Sphenolithus ciperoensis*, *Sphenolithus distentus* and *Sphenolithus predistentus* were the most important biostratigraphic markers for the section. The quantification of the nannofossils, enabled the division of the studied section into eight distinct intervals according to the fluctuation in paleoproxies values and diversity indices: Interval A (CP17: Rupelian): oligotrophic assemblage of warmer surface waters; Interval B (CP18: Rupelian): temperate assemblage of mesotrophic/eutrophic surface waters; Interval C (CP18 and CP19a: Rupelian/Chattian): oligotrophic assemblage of warmer surface waters; Interval D (CP19a and CP19b: Chattian): temperate assemblage of mesotrophic/eutrophic surface waters; Interval E (CP19b: Chattian): oligotrophic assemblage of warmer surface waters; Interval F (CP19b: Chattian): temperate assemblage of oligotrophic surface waters; Interval G (CP19b: Chattian): temperate assemblage of oligotrophic surface waters; and Interval H (CN1a: Chattian): temperate assemblage of eutrophic surface waters.
Keywords: Calcareous Nannofossils; Ceará Rise; Oligocene

Resumo

A Elevação Ceará é uma feição assísmica localizada no Oceano Atlântico Equatorial, entre a Planície Abissal Demerara e a Planície Abissal do Ceará, que representa uma área chave para a compreensão de fácies oceânicas profundas. Na área de Petróleo e Gás, a identificação de biozonas com base em nanofósseis calcários é importante para o posicionamento biocronoestratigráfico e entendimento da evolução deposicional de estratos sedimentares. O estudo da sucessão oligocênica com base em nanofósseis calcários na Elevação Ceará colaborou na detecção de inferências paleoecológicas para o Oceano Atlântico Equatorial durante o Oligoceno. Com o auxílio de um microscópio óptico de luz polarizada foram observadas, descritas e contabilizadas quarenta e quatro espécies em quinze amostras, o que permitiu o biozoneamento do Site 929A, que engloba as biozonas NP23, NP24, NP25 do zoneamento padrão para nanofósseis, assim como a biozona NP26 - *Clausicoccus fenestratus*, recentemente proposta. Dentre as espécies encontradas, destacam-se os *Sphenolithus ciperoensis*, *Sphenolithus distentus* e *Sphenolithus predistentus*, importantes marcadores bioestratigráficos do Oligoceno. Através da quantificação dos fósseis foi possível dividir a seção estudada em oito intervalos distintos, de acordo com as variações nos valores dos paleoproxies e dos índices de diversidade que refletem possíveis características paleoecológicas: Intervalo A (CP17: Rupeliano): associação típica de águas superficiais mais aquecidas e oligotróficas; Intervalo B (CP18: Rupeliano): associação típica de águas superficiais mais temperadas e mesotróficas/eutróficas; Intervalo C (CP18 e CP19a: Rupeliano/Chattiano): associação típica de águas superficiais mais aquecidas e oligotróficas; Intervalo D (CP19a e CP19b: Chattiano): associação típica de águas superficiais mais temperadas e mesotróficas/eutróficas; Intervalo E (CP19b: Chattiano): associação típica de águas superficiais mais aquecidas e oligotróficas; Intervalo F (CP19b: Chattiano): associação típica de águas superficiais mais temperadas e oligotróficas; Intervalo G (CP19b: Chattiano): associação típica de águas superficiais mais temperadas e oligotróficas; Intervalo H (CN1a: Chattiano): associação típica de águas superficiais mais temperadas e eutróficas.
Palavras-chave: Nanofósseis Calcários; Elevação Ceará, Oligoceno

1 Introduction

The calcareous nannofossils are widely used in biostratigraphic and paleoecological researches. This group has a number of advantages for those studies, such as the ease of sample preparation and the small size of these organisms, which contributes to the preservation of their entire hard skeletal tissues, presenting wide geographical distribution and high abundance values (Schneidermann, 1973). Due to its high recovery, population density, rapid evolution and planktonic nature, also reinforces the applicability of these organisms for age modeling (Antunes, 1997). According to Sezen (2014), the Ocean Drilling Program (ODP) Site 929A (Leg 154) was sampled in an immersed area of Ceará Rise, in the Equatorial Atlantic Ocean. The Leg 154 was proposed to elaborate a model of chemical evolution of the Cenozoic deep water working near Ceará Abyssal Plain and Ceará Rise, as well as near the Amazon Mouth Basin (Sezen, 2014).

This geomorphological feature is located under heated surface waters, which provides a great framework for the execution of this study, also providing conditions to conduct studies based on carbonate microfossils. Previous researches were conducted in this region, with well-calibrated dating for comparison of results (Sezen, 2014; Bergen *et al*., 2017; Blair *et al*., 2017; Boesiger *et al*., 2017; Browning *et al*., 2017; de Kaenel *et al*., 2017).

Therefore, this study aims to identify and quantify the assemblage of calcareous nannofossils recovered in fifteen samples from an Oligocene section of the ODP Leg 154, Site 929A, in the Ceará Rise, proposing and age model and inferring paleoecological conditions for the studied section.

2 Geological Setting

The Ceará Rise is an aseismic zone located in the Equatorial Atlantic Ocean with approximately 3000 meters deep, limited by the Ceará Abyssal Plain to the Southeast and the Amazon Mouth Basin to the Northwest. This feature is morphologically defined as an underwater topographic rise, located in the oceanic crust region (Curry *et al*., 1995).

According to Kumar & Embley (1977), the igneous basement of the Ceará Rise was formed around 80 my, during the Campanian, when the Mid-Atlantic Ridge, situated went through a period of intense volcanism. During the spreading of the ocean floor, the volcanic extrusion was divided into two distinct segments: the Ceará Rise was formed in the western side and the Sierra Leone Rise was formed in the eastern side (Figure 1).

The site 929A is located at the coordinates 5º58.573'N and 43º44.396'W, beneath warm surface waters of about 27ºC on the northwest flank of the Ceará Rise, under 4397 meters deep (Curry *et al*., 1995; Sezen, 2014). The section shows three stratigraphic units and the studied interval (unit III, illustrated in association with the paleoecological indices in Figure 6) consists mostly of clayey nanno-foram chalks (Curry *et al*., 1995).

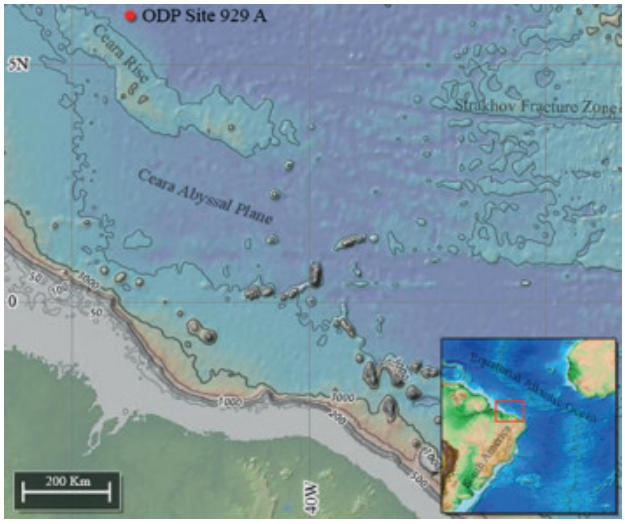

Figure 1 Site 929A location and main associated geomorphological features (adapted from NOAA, 2018)

3 Material and Methods

Fifteen samples were prepared according to the method described on Wanderley (2004). A polarized light optical microscope (*Zeiss*), with 1000x to 1600x total magnification, was used for the micropaleontological analysis. The identified *taxa* were classified based on the taxonomy described in Perch-Nielsen (1985), de Kaenel & Villa (1996), Bown (1998), Young *et al*. (2017), Bergen *et al*.

(2017), Boesiger *et al*. (2017) and de Kaenel *et al*. (2017), through four complete traverses of the coverslip (with polarized and natural lights). Ten fixed fields of view (FOV), without overlapping, were counted and relative abundances (RA%) were calculated for each sampled depth as described in Bown & Young (1998).

The quantified population was compiled into the main taxonomic and morphometric groups (*Clausicoccus* spp., *Coccolithus pelagicus* (<14 μm), *Coccolithus eopelagicus*, *Cyclicargolithus* spp., *Discoaster* spp., *Helicosphaera* spp., *Pontosphaera* spp., *Pyrocyclus* spp., *Reticulofenestra dictyoda*, *Reticulofenestra haqii* + *Reticulofenestra minuta*, *Reticulofenestra lockeri* + *Reticulofenestra daviesii*, *Reticulofenestra perplexa* + *Reticulofenestra bisecta*, *Sphenolithus* spp., *Thoracosphaera* spp. and *Triquetrorhabdulus* spp.), subsequently encompassed into paleoproxies (taxonomic groups with similar paleoecological signal): warm, temperate, cold, oligotrophic, meso-eutrophic, tropical and subtropical *taxa* as described in Haq & Lohmann (1976), Wei & Wise (1990), Gibbs *et al*. (2004), Persico & Villa (2004) and Villa *et al*. (2008).

4 Results and Discussion

Forty-four species and morphotypes were identified and illustrated (Figures 2, 3 and 4). The photomicrographs have been ordered according to the informal taxonomic groups described in Young *et al*. (2017).

4.1 Biostratigraphy

The reference biozonations used in this study were Martini (1971), Okada & Bukry (1980), and Agnini *et al*. (2014). The biozonation of Martini (1971) is based on the first and last occurrences of calcareous nannofossils from cores drilled by the Deep Sea Drilling Program (DSDP) in many latitudes (Bukry, 1973). This biozonation is represented, in this research, by the zones NP23, NP24, NP25, and NP26. Biozones of Okada & Bukry (1980) were based on data from the ODP, recovered in the Equatorial Atlantic Ocean, and, in this study, it's covered by the zones CP17, CP18, CP19a, CP19b, and CN1a. The biozonation of Agnini *et al*. (2014) is based on drilling sequences in deep sea areas at low and medium latitudes, as well as marine sections of the ancient Tethys Sea. This zonation is characterized, in this analysis, by the zones CNO3, CNO4, CNO5, and CNO6.

A new biozone was proposed by de Kaenel *et al*. (2017), referred as NP26, which is positioned at the top of Oligocene, between the top of NP25 biozone and the base of NN1 biozone. The NP26 was first studied by Martini (1971) and then amended by de Kaenel *et al*. (2017) so its lower limit has shifted to newer ages. Okada & Bukry (1980) revealed a "NP26" informal zone, corresponding to CN1 - *Cyclicargolithus abisectus*. This biozonation uses the higher occurrence of *Sphenolithus ciperoensis* (24.215 million years) as a consistent biohorizon for the base of this zone, as the the top is marked by the lower occurrence of *Discoaster druggi* (10-15 μm) in 23.155 million years (de Kaenel *et al*., 2017).

The studied section shows its base in Lower Oligocene - Rupelian (NP23 biozone) with average depth of 461 meters below sea floor. The top of the range is located in Upper Oligocene - Chattian (biozone NP26) with average depth of 335 meters below sea floor. The biozones in this work are in accordance with previous zonations of Curry *et al*. (1995) and Sezen (2014), for the same Leg, differing only in the detection of the recent described NP26 and the biozonation of Agnini *et al*. (2014) for the Site. All the detected zones and respective depths and ages were plotted with the nannofossils stratigraphic ranges in Figure 5.

4.2 Paleoecological Inferences

The calcareous nannofossil population studied at Site 929A was divided into eight intervals described according to the comparison of the RA% of the paleoproxies and diversity indices (Figure 6) as the number of individuals [N], species richness [S], dominance [D], equitability [J], and the Shannon diversity index [H]' (Shannon, 1948; McNaughton & Wolf, 1970; Gotelli & Colwell, 2001; Whittaker *et al*., 2001).

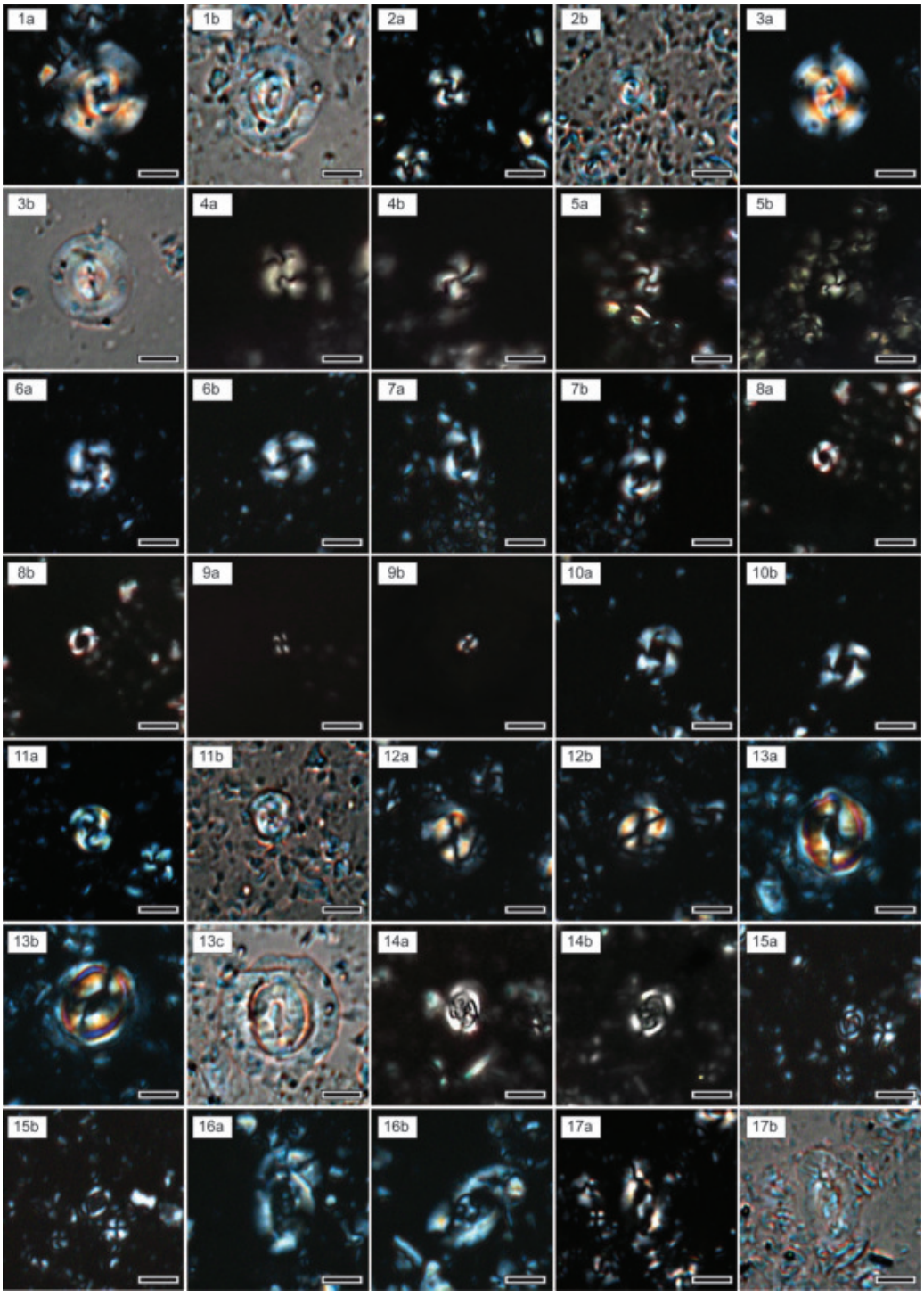

Figure 2 1a-b: *C. abisectus* (40-1, NP25), a) 90º/PL, b) 90º/NL; 2a-b: *C. floridanus* (43-1, NP24), a) 90º/PL, b) 90º/NL; 3a-b: *R. bisecta* (49-1, NP23), a) 90º/PL, b) 90º/NL; 4a-b: *R. perplexa* (45-1, NP23), a) 90º/PL, b) 45º/PL; 5a-b: *R. producta* (36-1, NP26), a) 90º/PL, b) 45º/PL; 6a-b: *R. daviesii* (37-1, NP25), a) 90º/PL, b) 45º/PL; 7a-b: *R. lockeri* (44-1, NP24), a) 90º/PL, b) 45º/PL; 8a-b: *R. haquii* (36-1, NP26), a) 90º/PL, b) 45º/PL; 9a-b: *R. minuta* (41-1, NP25), a) 90º/PL, b) 45º/PL; 10a-b: *R. dictyoda* (46-1, NP23), a) 90º/PL, b) 45º/PL; 11a-b: *P. orangensis* (41-5, NP25), a) 90º/PL, b) 90º/NL; 12a-b: *C. pelagicus* (40-1, NP25), a) 90º/PL, b) 45º/PL; 13a-c: *C. eopelagicus* (40-1, NP23), a) 90º/PL, b) 45º/PL, c) 90º/NL; 14a-b: *C. fenestratus* (49-1, NP26), a) 90º/PL, b) 45º/PL; 15a-b: *C. subdistichus* (38-1, NP25), a) 90º/PL, b) 45º/PL; 16a-b: *Helicosphaera* sp. (38-1, NP25), a) 90º/PL, b) 45º/PL; 17a-b: *H. intermedia* (43-1, NP24), a) 90º/PL, b) 90º/NL. Scale: 5 µm; PL: polarized light; NL: natural light.

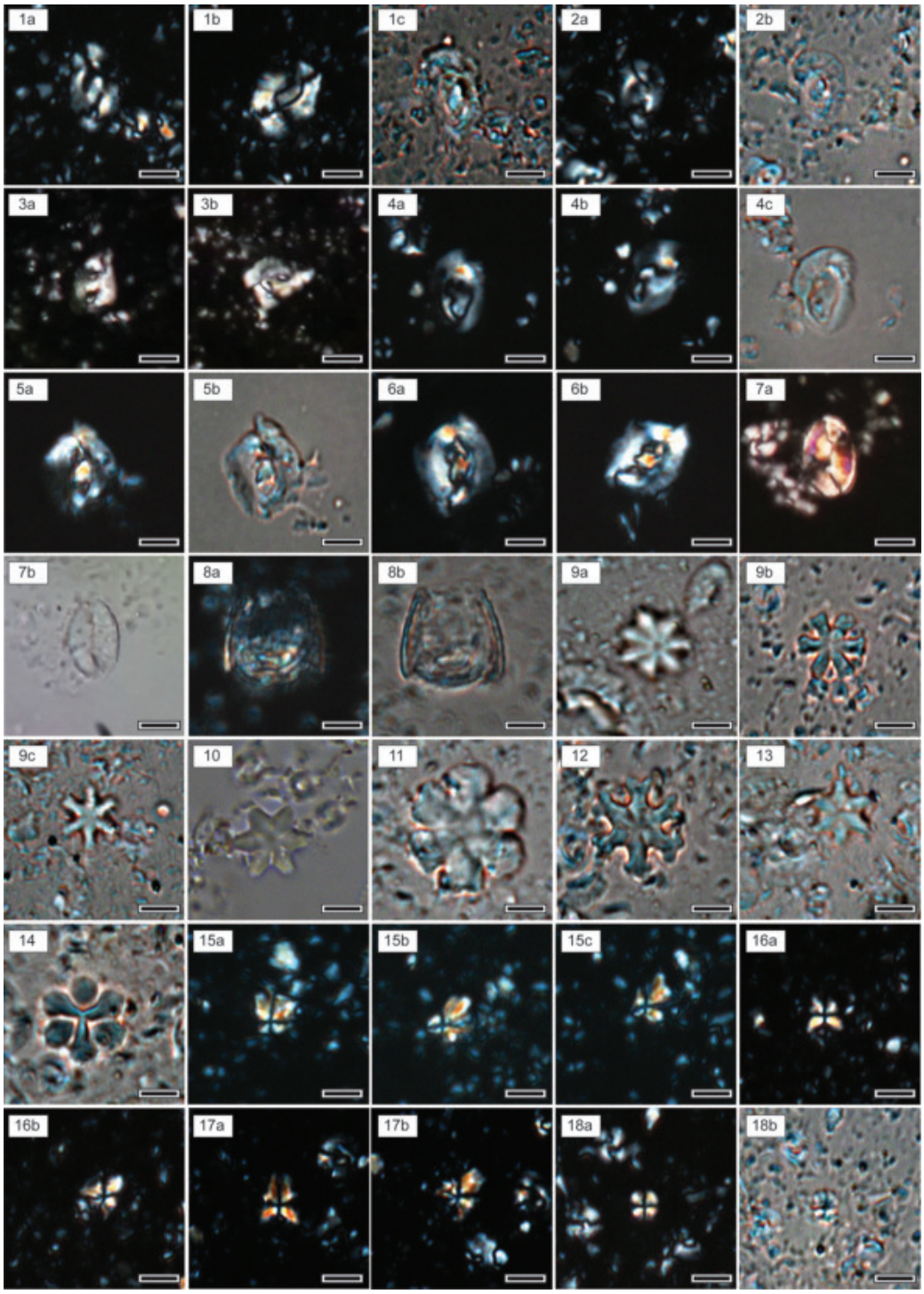

Figure 3 1a-c: *H. euphratis* (43-1, NP24), a) 90º/PL, b) 45º/PL, c) 90º/NL; 2a-b: *H. truempyi* (40-1, NP25), a) 90º/PL, b) 45º/PL; 3a-b: *H. recta* (45-1, NP23), a) 90º/PL, b) 45º/PL; 4a-c: *H. obliqua* (38-1, NP25), a) 90º/PL, b) 45º/PL, c) 90º/NL; 5a-b: *H. compacta* (47-1, NP23), a) 90º/PL, b) 90º/NL; 6a-b: *H. robinsoniae* (50-1, NP23), a) 90º/PL, b) 45º/PL; 7a-b: *Pontosphaera* sp. (37-1, NP25), a) 90º/PL, b) 90º/NL; 8a-b: *Syphosphaera* sp. (36-1, NP26), a) 90º/PL, b) 90º/NL; 9a-c: *Discoaster* sp. (41-1, NP25), a) 90º/NL, b) 90º/NL, c) 90º/NL; 10: *D. adamanteus* (38-1, NP25), 90º/NL; 11: *D. calculosus* (36-1, NP26), 90º/NL; 12: *D. deflandrei* (44-1, NP24), 90º/NL; 13: *D. druggi* (36-1, NP26), 90º/NL; 14: *D. trinus* (36-1, NP26), 90º/NL; 15a-c: *S. truaxii* (38-1, NP25), a) 90º/PL, b) 45º/PL; c) 45º/PL; 16a-b: *S. abies* (37-1, NP25), a) 90º/PL, b) 45º/PL; 17a-b: *S. apoxis* (36-1, NP26), a) 90º/PL, b) 45º/PL; 18a-b: *S. moriformis* (41-5, NP25), a) 90º/PL, b) 90º/NL. Scale: 5 µm; PL: polarized light; NL: natural light.

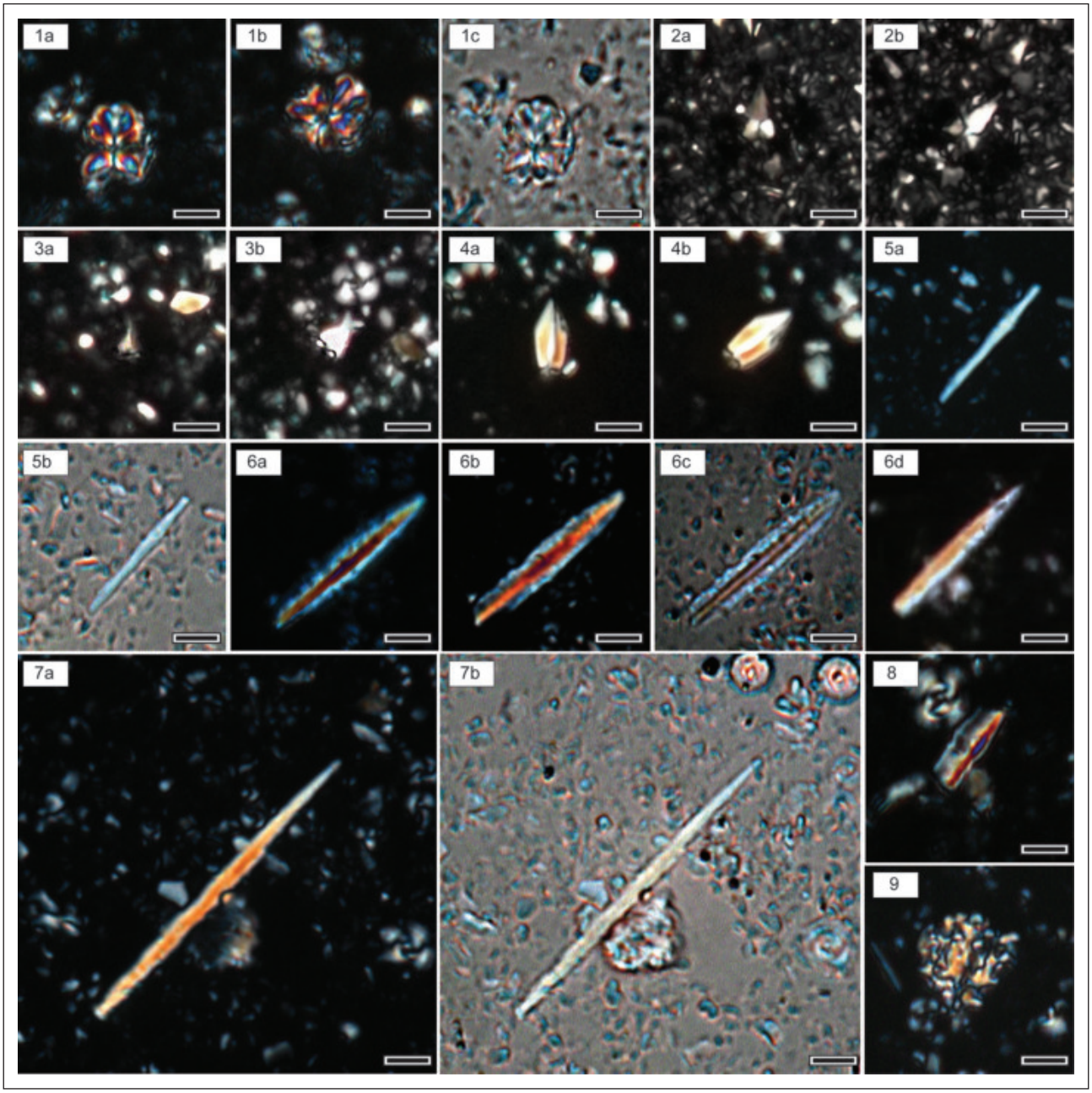

Figure 4 1a-c: *S. puniceus* (37-1, NP25), a) 90º/PL, b) 45º/PL, c) 90º/NL; 2a-b: *S. ciperoensis* (41-5, NP25), a) 90º/PL, b) 45º/PL; 3a-b: *S. distentus* (43-1, NP24), a) 90º/PL, b) 45º/PL; 4a-b: *S. predistentus* (46-1, NP23), a) 90º/PL, b) 45º/PL; 5a-b: *Triquetrorhabdulus* sp. (40-1, NP25), a) 45º/PL, b) 45º/NL; 6a-d: *T. carinatus* (40-1, NP25), a) 45º/PL, b) 45º/PL, c) 45º/NL, d) 45º/PL; 7a-b: *T. longus* (40-1, NP25), a) 45º/PL, b) 45º/NL 8: *T. milowii* (38-1, NP25), 45º/PL; 9: *Thoracosphaera* sp. (47-1, NP23), 90º/PL. Scale: 5 µm; PL: polarized light; NL: natural light.

Discoaster spp. and *Sphenolithus* spp. are generally considered as tropical warm and oligotrophic *taxa* (Gibbs et al., 2004; Villa *et al*., 2008). *Helicosphaera* spp. are adapted to warm coastal and platform environments, with high nutrient availability, being limited to low latitudes and shallow seas (Wei & Wise, 1990). *Cyclicargolithus* spp. does not show preferential temperature (Persico & Villa, 2004), but according to Wei & Wise (1990), this group is better suited to temperate environments

Anuário do Instituto de Geociências - UFRJ
ISSN 0101-9759 e-ISSN 1982-3908 - Vol. 43 - 1 / 2020 p. 07-17

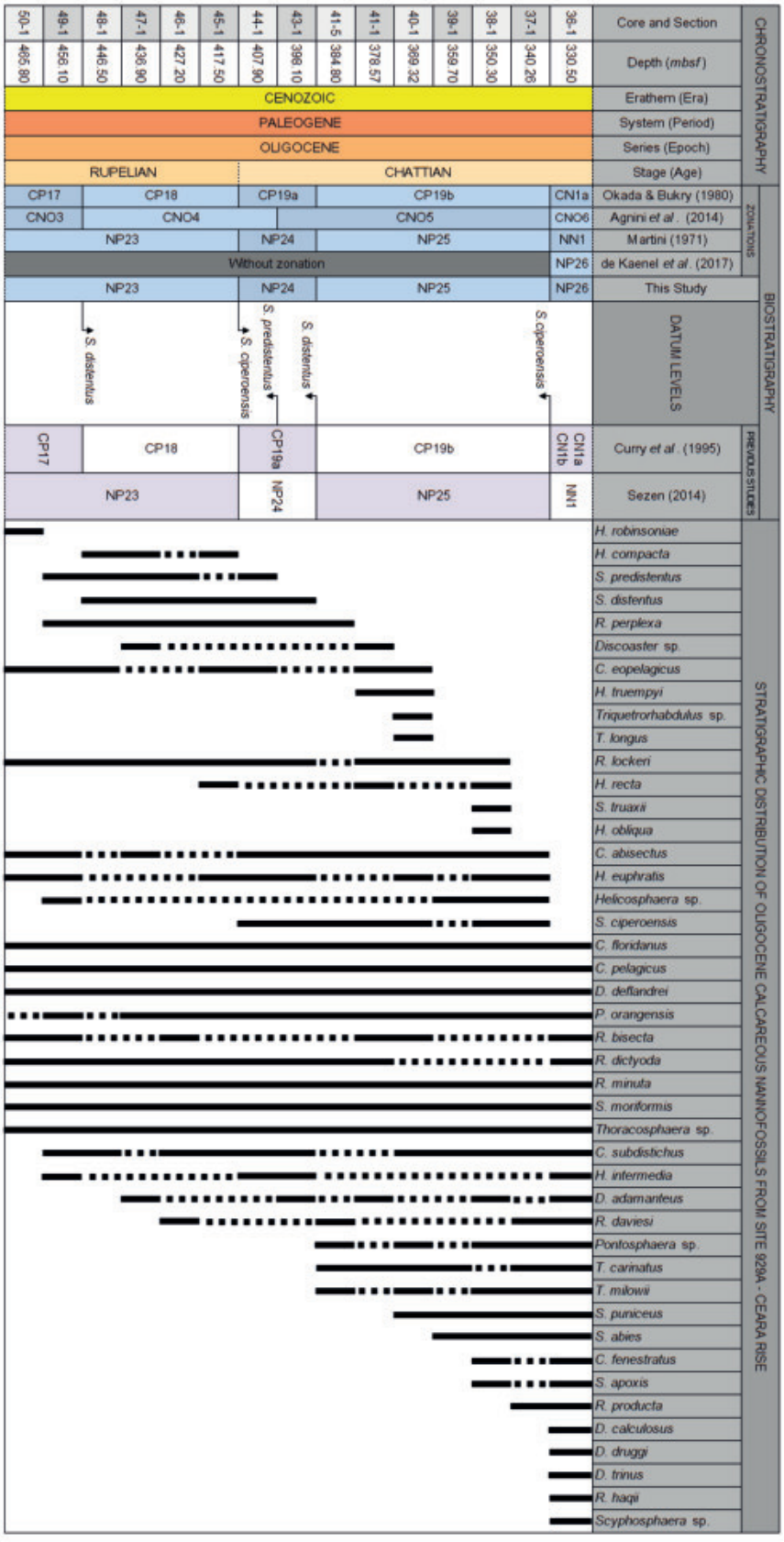

Figure 5 Calcareous nannofossils biostratigraphic distribution for Site 929A. Species organized in order of last occurrences.

and medium latitudes. *R. bisecta* is adapted to low and medium latitudes, preferring temperate waters (Wei & Wise, 1990). However, results from Haq & Lohmann (1976) characterized the species as high latitudes *taxa*.

Reticulofenestra daviesii and *C. pelagicus* are adapted to eutrophic cold waters from high to medium latitudes, evidenced by the increase in the number of individuals during the Oi-1 (Oxygen Isotope Event) cooling event in the Oligocene, and *Reticulofenestra* spp. ≤ 4 μm could indicate heated meso-eutrophic waters (Persico & Villa, 2004).

This comparative dataset enabled the identification of eight intervals of paleoecological trends, as described below in chronological order:

Interval A: occurs in samples 49-1 and 50-1 (CP17: Rupelian), showing a typical assemblage of warmer oligotrophic surface waters, composed of subtropical species, associated with the increase of richness, number of individuals, equitability and Shannon diversity and decrease of dominance, suggesting favorable conditions to nannoplankton development.

Interval B: occurs between the samples 46-1 and 49-1 (CP18: Rupelian), showing a typical assemblage of temperate mesotrophic/eutrophic surface waters, composed of subtropical latitude species, associated with the increase of dominance and decrease of richness, number of individuals, equitability and Shannon diversity, suggesting some influence of terrigenous input.

Interval C: occurs between the samples 44-1 and 46-1 (CP18 and CP19a: Rupelian/Chattian), showing a typical assemblage of warmer oligotrophic surface waters, composed of tropical latitude species, associated with the increase of richness, number of individuals, equitability and Shannon diversity values and decrease of dominance, suggesting favorable conditions to nannoplankton development.

Interval D: occurs between the samples 44-5 and 44-1 (CP19a and CP19b: Chattian), showing a typical assemblage of temperate mesotrophic/eutrophic surface waters, composed of subtropical latitude species, associated with the increase of the number of individuals, equitability and Shannon diversity, associated with low decrease of richness and dominance, showing week evidence of eutrophic opportunism.

Interval E: occurs between the samples 40-1 and 41-5 (CP19b: Chattian), showing a typical assemblage of warmer oligotrophic surface waters, composed of tropical species, associated with the increase of richness, number of individuals and dominance, and decrease of equitability and Shannon diversity, which could indicate an abrupt input of warmer surface waters, with strong indicators of increased nutrient levels in the lower portion of the interval, and stabilization of paleoceanographic conditions in the upper portion.

Interval F: occurs in the samples 39-1 and 40-1 (CP19b: Chattian), showing a typical assemblage of more temperate oligotrophic surface waters, composed of subtropical latitude species, associated with the increase of dominance and decrease of richness, number of individuals, equitability and Shannon diversity, suggesting a possible transitional environment between warm and cold surface waters, with gradual increase in eutrophic indicators, pointing out a possible establishment of opportunistic populations.

Interval G: occurs between the samples 37-1 and 39-1 (CP19b: Chattian), showing a typical assemblage of temperate oligotrophic surface waters, composed of typical subtropical latitude species, associated with the increase of richness, equitability and Shannon diversity, and decrease of the number of individuals and dominance, suggesting a transitional surface water environment with possible fluctuation and mixing between higher trophic levels at the base and top of the interval with the central portion with decreased nutrient levels.

Interval H: occurs in samples 36-1 and 37-1 (CN1a: Chattian), showing a typical assemblage of temperate eutrophic surface waters, composed of subtropical species, associated with the increase of richness, number of individuals, equitability and Shannon diversity, and decrease of dominance, suggesting a possible colder surface water environment and increased nutrient levels due terrigenous input or increased influence of deep thermohaline water masses (upwelling).

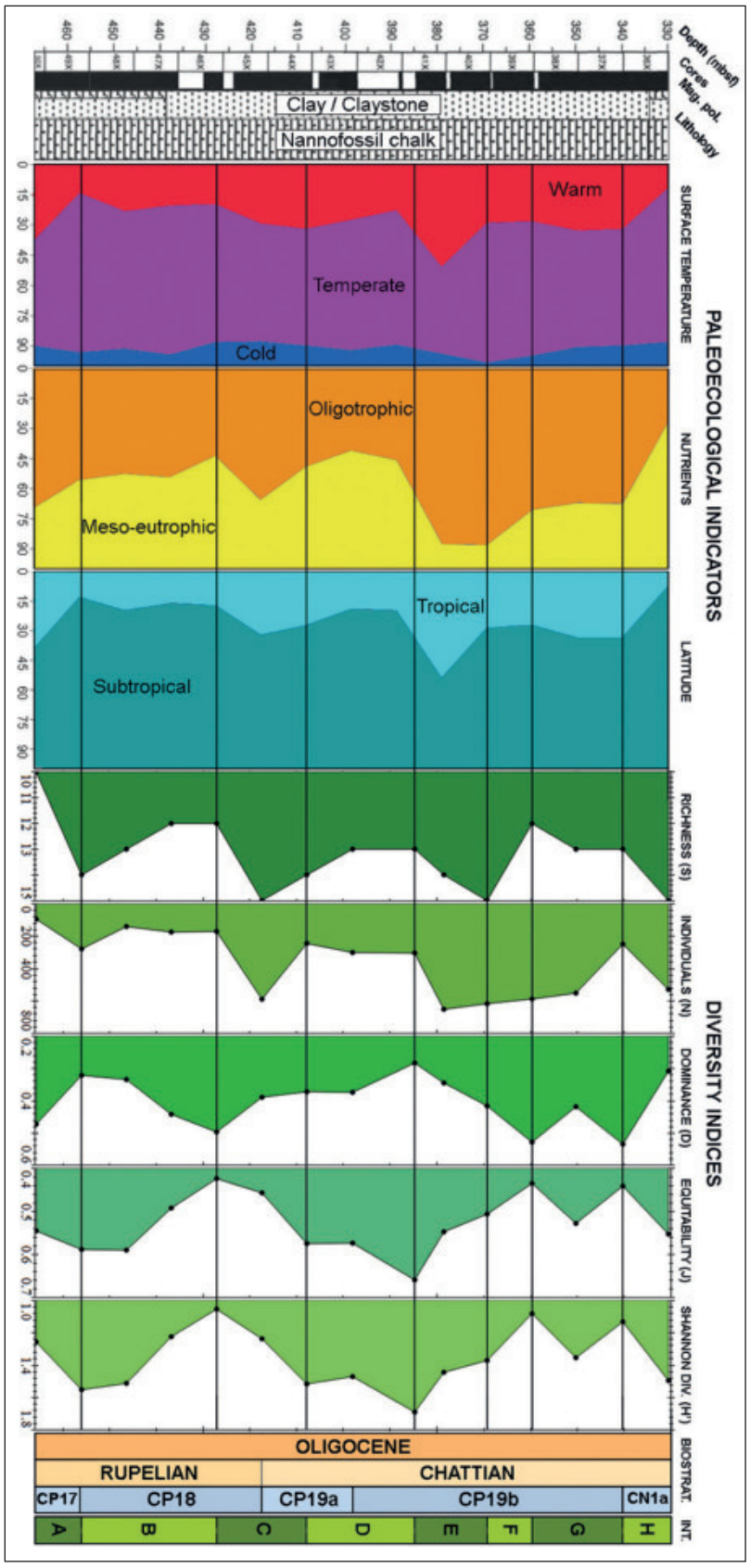

Figure 6 Paleoecological indices and paleoproxies RA% values for the site 929A

5 Conclusions

The qualitative and quantitative calcareous nannofossil analysis of the ODP 929A Oligocene section enabled the identification of forty-four species, with three biostratigraphic markers (*S. ciperoensis, S. distentus* and *S. predistentus*) and four standard biozones: NP23, NP24, NP25 (Martini, 1971) and NP26 (de Kaenel *et al.,* 2017), equivalent to the zones CP17, CP18, and subzones CP19a, CP19b and CN1 (Okada & Bukry, 1980), and CNO3, CNO4, CNO5 and CNO6 (Agnini *et al*., 2014). In this research, the recently proposed biozone NP26 - *Clausicoccus fenestratus* (de Kaenel *et al*., 2017) was detected in sample 36-1 (≅ 330,50 mbsf) of the studied section, marking the Uppermost Oligocene, between the NP25 and NN1 zones. The most common *taxa* (*Clausicoccus* spp., *C. pelagicus* (<14 μm), *C. eopelagicus*, *Cyclicargolithus* spp., *Discoaster* spp., *Helicosphaera* spp., *Pontosphaera* spp., *Pyrocyclus* spp., *R. dictyoda*, *R. haqii* + *R. minuta*, *R. lockeri* + *R. daviesii*, *R. perplexa* + *R. bisecta*, *Sphenolithus* spp., *Thoracosphaera* spp. e *Triquetrorhabdulus* spp.) and quantified, allowing a comparative interpretation of the paleoproxies and diversity index, enabling the division of the section into eight intervals (A-H), which reflects fluctuations in temperature and nutrient levels of surface waters, setting a cyclicity of these parameters all through the Oligocene in the Ceará Rise.

Finally, we suggest the comparison between the quantification of calcareous nannofossils in higher sample resolutions, with the comparative quantification of dissolution levels of coccoliths and nannoliths, for future researches, in order to identify intervals of greater interference of diagenetic effects on the paleoecological signal.

6 Acknowledgements

The authors would like to thank the Ocean Drilling Program (ODP) for the samples, the Sedimentary Geology Laboratory (LAGESED-UFRJ) for the photomicrographs and Dr. Cleber Fernandes Alves (LAFO/UFRJ) for the critical reading and review that enriched the manuscript.

7 References

Agnini, C.; Fornaciari, E.; Raffi, I.; Catanzariti, R.; Pälike, H.; Backman, J. & Rio, D. 2014. Biozonation and biochronology of Paleogene calcareous nannofossils from low and middle latitudes. Newsletters on Stratigraphy, 47: 131-181.

Antunes R.L. 1997. Introdução ao Estudo dos Nanofósseis Calcários. Rio de Janeiro, Universidade Federal do Rio de Janeiro, Série didática, 115p.

Bergen, J.; De Kaenel, E.; Blair, S.; Boesiger, T. & Browning, E. 2017. Oligocene-Pliocene Taxonomy and Stratigraphy of the genus Sphenolithus in the Circum North Atlantic Basin: Gulf of Mexico and ODP Leg 154. Journal of Nannoplankton Research, 37 (2-3): 77-122.

Blair, S.; Bergen, J.; De Kaenel, E.; Browning, E. & Boesiger, T.M. 2017. Upper Miocene-Lower Pliocene taxonomy and stratigraphy in the circum North Atlantic Basin: radiation and extinction of Amauroliths, Ceratoliths and the D. quinqueramus lineage. Journal of Nannoplakton Research, 37(2-3): 113-144.

Boesiger, T.M.; De Kaenel, E.; Bergen, J.A.; Browning, E.; & Blair, S.A. 2017. Oligocene to Pleistocene taxonomy and stratigraphy of the genus Helicosphaera and other placolith taxa in the circum North Atlantic Basin. Journal of Nannoplankton Research, 37 (2-3): 145-175.

Bown, P.R. 1998. Calcareous nannofossil biostratigraphy. Cambridge, British Micropalaeontological Society Publication Series, Chapman & Hall, 328p.

Bown, P.R. & Young, J.R. 1998. Techniques. In, BOWN, P.R. (ed.) Calcareous Nannofossil Biostratigraphy. British Micropalaeontological Society Publication Series, 16-28.

Browning, E.; Bergen, J.A.; Blair, S.A.; Boesiger, T.M. & de Kaenel, E. 2017. Late Miocene to Late Pliocene taxonomy and stratigraphy of the genus Discoaster in the circum North Atlantic Basin: Gulf of Mexico and ODP Leg 154. Journal of Nannoplankton Research, 37(2-3): 189-214.

Bukry, D. 1973. Low-latitude coccolith biostratigraphic zonation. In: EDGAR, N.T.; SAUNDERS J.B. et al. (eds.) Initial Report Deep Sea Drilling Project, 15: 685-703.

Curry, W.B.; Shackleton, N.J.; Richter, C.; et al. 1995. Proc. ODP, Init. Reptorts. College Station, TX (Ocean Drilling Program), 337-417.

De Kaenel, E.; Bergen, J.A.; Browning, E.; Blair, S.A. & Boesiger, T.M. 2017. Uppermost Oligocene to Middle Miocene Discoaster and Catinaster taxonomy and stratigraphy in the circum North Atlantic Basin: Gulf of Mexico and ODP Leg 154. Journal of Nannoplankton Research, 37(2-3): 215-244.

De Kaenel, E. & Villa, G. 1996. Oligocene-Miocene calcareous nannofossil biostratigraphy and paleoecology from the Iberian Abyssal Plain. Proceedings of the Ocean Drilling Program. Scientific Results, 149: 79-145.

Gibbs, S.J.; Shackleton, N.J. & Young, J.R. 2004. Identification of dissolution patterns in nannofossil assemblages: A high-resolution comparison of synchronous records from Ceara Rise, ODP Leg 154. Paleoceanography, 19(1): 1-12.

Gotelli, N.J. & Colwell, R.K. 2001. Quantifying biodiversity: procedures and pitfalls in the measurement and comparison of species richness. Ecology Letters, 4(4): 379-391.

Haq, B.U. & E Lohmann, G.P. 1976. Early Cenozoic calcareous nannoplankton biogeography of the Atlantic Ocean. Marine Micropaleontology, 1:119-194.

Kumar, N. & Embley, R.W. 1977. Evolution and origin of Ceará Rise: An aseismic rise in the western equatorial Atlantic. Geol. Soc. America Bull., 88: 683-694.

Martini, E. 1971. Standard tertiary and quaternary calcareous nannoplankton zonation. In: CONFERENCE OF PLANKTON MICROFOSSILS, 2, Rome, 1970. Proceedings of the second planktonic conference, Edizione Tecnoscienza, Rome, p. 737-785.

McNaughton, S.J. & Wolf, L.L. 1970. Dominance and the Niche in Ecological Systems.Science. 167(3915): 131-139.

NOAA. 2018. Curators of Marine and Lacustrine Geological Samples Consortium: Index to Marine and Lacustrine Geological Samples (IMLGS). NOAA National Centers forEnvironmental Information. Available in: <https://maps.ngdc.noaa.gov/viewers/sample_index/>. Access: 14 Nov. 2018.

Okada, H. & Bukry, D. 1980. Supplementary modification and introduction of code numbers to the low latitude coccolith biostratigraphy zonation (Bukry, 1973; 1975). Marine Micropaleontology, 5: 321-325.

Perch-Nielsen, K. 1985. Mesozoic calcareous nannofossils / Cenozoic calcareous nannofossils. In: BOLLI H.M., SAUNDERS J.B., PERCH-NIELSEN K. (eds.) Plankton Stratigraphy. Cambridge University Press, Cambridge. p. 329-554.

Persico, D. & Villa, G. 2004. Eocene-Oligocene calcareous nannofossils from Maud Rise and Kerguelen Plateau (Antarctica): paleoecological and paleoceanographic implications. Marine Micropaleontology, 52(1-4): 153-179.

Schneidermann, N. 1973. Deposition of coccoliths in the compensation zone of the Atlantic Ocean. In: CALCAREOUS NANNOFOSSIL SYMPOSIUM. Houston, p. 140-151.

Sezen, T. 2014. Oligocene-Lower Miocene Calcareous Nannofossil Biostratigraphy of ODP Leg 154 Hole 929A from the Western Equatorial Atlantic at the Ceará Rise. College of Arts and Sciences, Florida State University. Dissertation, Master of Science, 70p.

Shannon, C.E. 1948. A mathematical theory of communication. The Bell System Technical Journal, 27, 379-423.

Villa, G.; Fioroni, C.; Pea, L.; Bohaty, S. & Persico, D. 2008. Middle Eocene-late Oligocene climate variability: Calcareous nannofossil response at Kerguelen Plateau, site 748. Marine Micropaleontology, 69(1): 173-192.

Wanderley, M.D. 2004. Nanofósseis Calcários. In: CARVALHO I.S. (ed.) Paleontologia. Editora interciência, p. 285-296.

Wei, W. & Wise, S.W. 1990. Biogeographic gradients of middle Eocene-Oligocene calcareous nannoplankton in the South Atlantic Ocean. Palaeogeography, Palaeoclimatology, Palaeoecology, 79(1-2): 29-61.

Whittaker, R.J., Willis, K.J. & Field, R. 2001. Scale and species richness: towards a general, hierarchical theory of species diversity. Journal of Biogeography, 28(4): 453-470.

Young, J.R.; Bown P.R. & Lees J.A. 2017. Nannotax3 website. International Nannoplankton Association. Disponível em: <http://www.mikrotax.org/Nannotax3>. Access in: Mar. 2016 - Nov. 2018>.